E-ISSN 2581 – 7957
P-ISSN 2277 – 3916

CVR Journal of Science and Technology, Volume 22, June 2022
DOI: 10.32377/cvrjst2214

The Phase Transformation of Low Carbon Steel using Controlled Cooling Systems

Dr.Manjeet Kharub
Assoc. Professor, CVR College of Engineering/Mechanical Engg. Department, Hyderabad, India
Email: manjeetkharub@gmail.com

Abstract: **Automobile manufacturers face mounting pressure to develop new materials that improve their vehicles' fuel economy, pollution emissions, and crash safety. These objectives appear ambiguous when they must be met while reducing the weight of a vehicle. This requires using materials with a high strength-to-weight ratio and high formability. The objectives of the work presented in this paper were to control the cooling of steel with lean chemistry to generate a multi-functional multi/dual-phase steel. The calculations were performed using JMat-Pro and Thermo-Calc. The CCT, TTT, equilibrium diagram, and phase fraction diagram of the steel is under investigation. It was found that inter-critical annealing can be achieved with a variety of strength-ductility combinations in steels with proper cooling pathways. Therefore, by modifying the heat treatment parameters, the examined steel's alloy chemistry enabled the achievement of a wide variety of strengths and ductility combinations.**

Index Terms: **dual-phase (DP) steels, heat treatment, annealing, phase transformation, control cooling**

I. INTRODUCTION

Engineers and scientists have developed a new class of steels specifically for vehicles [1]. Compared to traditional mild steel, these steels are designed to meet stringent safety and emissions regulations and the requirements of today's vehicles at a modest rate [2]. These steels are approximately six times more resistant to corrosion than those used earlier. They are known as Advanced High-Strength Steels (AHSS) and are more sophisticated, complex materials [3]. These steels also provide a higher strength-to-weight ratio without sacrificing durability, ductility, or formability with a carefully chosen chemical composition. They exhibit a better strength-to-elongation ratio than conventional steels due to their dual/multiphase crystallites caused by conventional cooling or controlled cooling of steels with high chemistry (high alloy content) [4]. Because processing of chemistry-rich steels is expensive, the objective of cost-effectiveness was never met using these steels. Various processing techniques have been described in the relevant literature, the majority of which employ standard cooling methods from the heat treatment processes [5]. Few authors have reported on manufacturing these steels using controlled cooling ideas but have instead used steels with rich chemistry to achieve the necessary attributes. Also, the cost-efficiency target is not attained with significant alloy content in these steels. Therefore, the primary goal of this study was to develop multi-functional steels with dual/multiphase microstructures generated by controlled cooling of low carbon steel. Microstructures with many phases were created in low normalized carbon steel (0.11C, 1.8Mn, and 0.325 Si) by adjusting inter-critical annealing settings in an annealing simulator. Thus, this paper makes an effort to employ steels with low carbon content and treat them utilizing controlled cooling techniques. Dual-phase microstructures were obtained by inter-critical annealing followed by quick cooling to ambient temperature, while multiphase microstructures were obtained by maintaining the bainitic and martensitic temperature ranges, respectively The present research work is an effort to address the following:

- To study the formation and stabilization of the austenite phase during inter-critical (isothermal) annealing of normalized steel under fast heating rates (up-quenching).
- To establish the process routes for the annealing cycle to produce the required multi/dual phase microstructures. The overall objective of the present work consisted of several sub-problems/ issues.

II. LITERATURE REVIEW

This section contains brief background knowledge based on the literature on the different methods used by past scholars to manufacture third-generation dual-phase steels and enhance their qualities.

Seong et al. [6] investigated the influence of retained austenite and the quantity of soluble carbon in TRIP (Transformation Induced Plasticity) steels on their mechanical characteristics. Two cold-rolled strips, CS1 (C-.077, Si-1.00, Mn-1.50, P-0.0084, and Sol. Al-0.036) and CS2 (C-0.079, Si-1.51, Mn-1.50, P-0.0095, and Sol. Al-0.033), each having a thickness of 1.3 mm, were heat treated. The heat treatment procedure included 50 seconds of austenitizing at 830 °C, fast cooling to the bainitic transition temperature of 360–460 °C, and 5 minutes of isothermal holding (austempering). In CS1 steel specimens, it was noticed that the retained austenite concentration dropped when the austempering temperature was increased. This occurred because increasing the austempering temperature resulted in cementite precipitation, which resulted in a quicker drop in the carbon content of residual austenite, facilitating the nucleation of new bainitic ferrite plates. The silicon-rich CS15 sample inhibited carbide production during bainite transformation, enriching the residual austenite with carbon. The authors found that increasing the austempering temperature reduced the amount of retained austenite and carbon. Additionally, the quantity of kept austenite was related to its carbon content, and elongation increased as retained austenite, and carbon content rose.

Hulka [7] examined the influence of niobium addition on the characteristics of Multi-Phase (MP/TRIP) steels. When MP steel was manufactured, the initial heat treatment was

Received on 18-03-2022, Revised on 07-05-2022, Accepted on 31-05-2022.

performed at a slightly higher temperature in the two-phase zone (50% ferrite and 50% austenite by wt). Quenching was enacted to prevent the production of significant ferrite—the final transition isothermally in the bainite zone (second heat treatment). Carbon spread into the remaining austenite islands during bainite production, eventually enriching them to a level of more than 1% carbon. It was observed that austenite containing a large amount of carbon was also stable at room temperature. Additionally, austenite may be stabilized at room temperature with the addition of niobium to multiphase steels.

According to Fang et al. [8], the addition of niobium alters the microstructure and mechanical properties of the material. It shortens the annealing time, resulting in increased retained austenite at room temperature due to carbon enrichment of austenite; the formation of NbC precipitates, which inhibit grain growth, results in fine-grained austenite. Additionally, Nb retards austenite recrystallization during hot strip rolling. So, by preparing additional nuclei for the austenite to ferrite transition, the grain size of the hot band was reduced. Thus, the parameters discussed above enhanced both strength (as a result of grain refining and NbC precipitation) and length (due to stability of austenite at room temperature and also by nucleation of ferrite at austenite-ferrite inter-phase during cooling).

After solidification, the slabs were hot-rolled and forged to produce rods with a 24x24mm section. The specimens were heated in three different ways. In routes I and II, the steel was heated to 910 °C (+ area) and held there for 30 minutes. In route I, the specimen was chilled to room temperature, then reheated to 750 °C and quenched with water. In route II, the specimen was quenched with water at both 910 °C and 750 °C. Method III entails austenitizing steel at 910 °C and then air cooling to 750 °C for 45 seconds to complete the partial transformation, followed by water quenching. The steel that had been heat-treated according to route I has a ferrite structure with an uneven martensite envelope at grain boundaries. In route II, austenite nucleation occurs mostly on the borders of martensite laths generated following initial quenching from a temperature of 910 °C. The predominating martensite component is found mainly as thin fibres at grain boundaries.

Additionally, tiny grains of recrystallized ferrite may be seen in the vicinity of martensite, particularly near the border zone of big grains of the alpha phase. Martensite was discovered on the grain boundaries of the alpha phase along route III. After 45 seconds of air cooling, the optimal martensite percentage of 20% occurs. The heat treatment parameters utilized resulted in the formation of DP-type steels with equivalent ferrite and martensite percentages. The optimal martensite fraction was found between 21% and 24%, and the phase grain size was between 7m and 10m. The varied shape of martensite has an effect on the steel's diverse mechanical characteristics and deformability.

The route II steel had the optimal strength and ductility. This steel had a yield point of about 520 MPa, a tensile strength of approximately 800 MPa, a total elongation of 20%, and uniform elongation of around 16%. Ahmad et al. (2007) investigated the influence of thermomechanical processing on the hardenability and tensile fracture characteristics of dual-phase (DP) steels. Thermo-mechanical processing with varied rolling reductions (0-50%) was used to quench low alloy hot rolled steel (0.09 C, 1.2 Mn, 0.78 Cr, 0.26 Si, 0.15 Ni, 0.2 Cu, 0.04 Mo, and balance Fe, percent wt) in the intercritical temperature range of 725–830 °C. The steel as received had a microstructure composed of ferrite and pearlite phases, as determined by the metallographic investigation. Inter-critical samples were heated for 20 minutes in an argon atmosphere to a temperature range of 725–830 °C and then quenched in a brine solution. Due to the rapid cooling rate, the austenite phase changed nearly entirely into martensite. The volume percent of austenite was determined using the point-counting technique. At a temperature of 790 °C, about 50% of austenite was created; at this temperature, samples were rolled, and cross-section reductions of 0–50% (0, 20, 30, and 50% reductions in the lateral and longitudinal directions) were attained. All specimens were quenched in an ice-cold brine solution, which provided a cooling rate of about 500 °C /s. Following grinding and polishing, specimens were etched with 5% picral solution, followed by 2% nital solution, and then submerged in a boiling alkaline chromate solution (8g $CrO3$ + 40g NaOH + 72 ml $H2O$). It was discovered that while rolling at a temperature of 790 °C for a thickness reduction of 0 to 50%, about 6% of ferrite increased in rolled specimens but not in un-rolled specimens, indicating that rolling in the inter-critical area lowered hardenability.

The increased rolling reduction resulted in increased strain, resulting in more fibrous martensite particles. Rolling extended and thinned the martensite fibres in the longitudinal direction, and they did not lengthen in the transverse direction, but widened in the direction corresponding to the rolling plane. Thus, the aspect ratio of the martensite fibres was greater in the longitudinal direction than in the transverse direction, which had a significant effect on the tensile characteristics. Total elongation was also considerably impacted by 50% rolling in the transverse and longitudinal directions, resulting in total elongation of 13% and 18%, respectively. Hot rolling at the inter-critical area boosted the steel's strength without sacrificing its ductility significantly. Additionally, rolling enhanced the aspect ratio of the martensite in the longitudinal direction more than in the transverse direction, resulting in the development of tensile characteristics.

Zhao et al. [2021] developed a novel approach for processing DP steel in which a sample of 0.17C-0.74Mn steel was treated in five phases to generate ultrafine-grained DP steel. After 30 minutes of soaking, the sample was quenched in an ice-brine solution, resulting in a completely martensite microstructure that was tempered in the second stage. In the third phase, the sample was cold rolled to an extent of 80 percent. In the fourth phase, the sample was annealed to 550 °C and soaked for 75 minutes before being quenched in water to create an ultrafine aggregate of ferrite and carbide. In step five, a system was quickly heated at a rate of 300 °C/s to a temperature between Ac1 and Ac2 and then soaked for 5–10 seconds to decrease ferrite grain development and enhance carbide dissolution and austenite production. On water quenching, an ultrafine structure with a martensite volume percentage of about 0.42 was formed with a uniform distribution of 2 um martensite islands.

For manufacturing TRIP steel, the authors advocated using nitrogen as an austenite stabilizer to enhance mechanical qualities; however, 200 ppm N2 was recommended for traditional steelmaking due to nitrogen's limited solubility. A significant degree of retained austenite stabilization occurs due to the high nitrogen concentration. The authors concluded that steels with desirable qualities would have a high proportion of austenite and high strength elements such as martensite, bainite, and ultrafine-grained ferrite.

III. EXPERIMENTAL PROCEDURE

The following information outline the experimental approach used in this study work:

A. Analytical characterization of the material that was received

A sheet of normalized steel, 1.0 mm thick, with the chemical composition described in Table 1 was used as a starting point.

TABLE I.
CHEMICAL COMPOSITION OF THE AS-RECEIVED STEEL

element	C	Mn	Si	S	P	Al	N	Fe
%wt.	0.11	1.8	0.325	0.006	0.016	0.052	0.0056	Rest

Standard metallographic processes such as mounting, planar grinding, rough polishing, final polishing, etching, etc. were used to prepare specimens of the as-received steel for microstructural investigation. The specimens were etched using Nital, a solution of HNO3 (3 percent) in ethanol. For varying levels of detail, images were captured using an optical microscope.

B. Software to Conduct Research on Phase Transformation

For heat-treated steel, annealing parameters needed to be determined once microstructure analysis was completed on the raw material. As a result, the focus of this stage of the study was on the specifics of the steel's annealing temperature range (the lower and higher critical temperatures), soaking times, cooling rates, and other cooling parameters. JMat-Pro and Thermo-Calc were used to do these calculations. The steel under investigation's CCT (continuous cooling transformation), TTT (time-temperature transformation), equilibrium diagram, and phase fraction diagram were all calculated using the software programmes.

C. Heat Treatment and Microstructural Analysis

Thermo-Calc and JMat-Pro software were used to compute process parameters for annealing tests. There were two kinds of samples used in the annealing process. Samples for the muffle furnace were produced as normal dog-bone specimens with 35-mm gauge length, whereas samples for the annealing simulator were created as 10-by-10-by-1-mm^3 samples. After heating in the muffle furnace and quenching with water, the quantity of austenite formed in the specified steel was determined by conducting annealing tests.

Different cooling methods were used in annealing simulator tests. Simulated alternative cooling paths were created by varying the concentrations and pressures of hydrogen and nitrogen gases fed into the simulator. Samples were annealed in the temperature range of Ac1–Ac3 for 3 minutes at various inter-critical temperatures and then cooled. This study employed the holding times described by Thomas et al. [10]. Water quenching was used as the cooling technique for muffle furnace samples, and samples were cooled following the CCT diagram for annealing simulator treatment. The resulting microstructures were distinct for each of the three cooling procedures (A, B, and C in Fig. 1).

There were martensite/ferrite microstructures in samples of type A that were immediately cooled (at a rate greater than critical cooling rate) to room temperature. Microstructures of type B samples were obtained by quickly cooling and holding them in the bainitic zone for one minute. To temper, the martensite, samples of type C were immediately cooled to a temperature between M_S and M_F and maintained there for one minute. Even before the samples were loaded, the heating chamber of the annealing simulator was pre-charged with a combination of hydrogen and nitrogen gases to guard against sample oxidation in a reducing atmosphere.

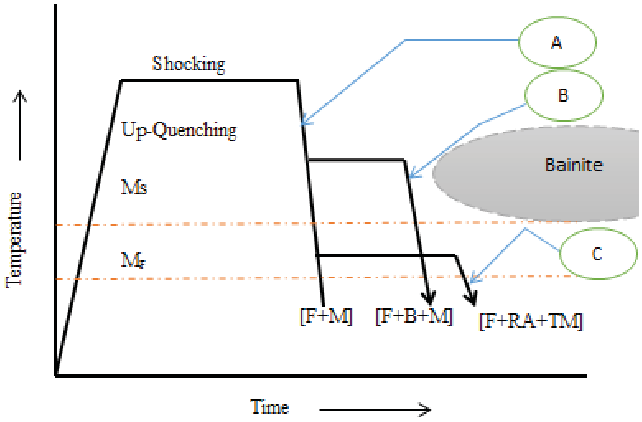

Figure 1. Schematic of different heat treatment routes

IV. RESULTS AND DISCUSSION

A. Microstructure of Material as received

With an average grain size of 15 micrometres, the microstructure of the obtained steel is composed of pro-eutectoid ferrite (88%) and pearlite (12%). See Fig. 2 for further information.

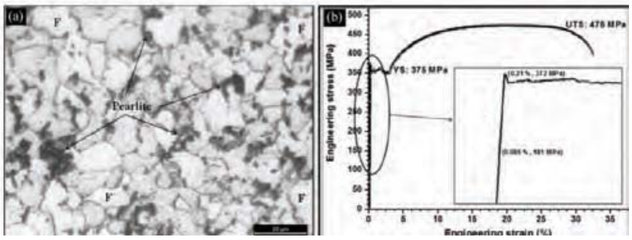

Figure 2. optical micrograph and tensile curve for the received steel

B. Process Parameter Predictions Using Software

The as-received normalized steel's equilibrium phase diagram and phase fraction diagram were constructed using Thermo-Calc software (See Fig. 3), which anticipated the Ac_1 and Ac_3 temperatures to be 684 °C and 834 °C, respectively. Using JMat-Pro, a CCT diagram for each annealing temperature was created. As indicated below, JMat-Pro predictions were used to calculate the proportion of austenite available for transformation into various products.

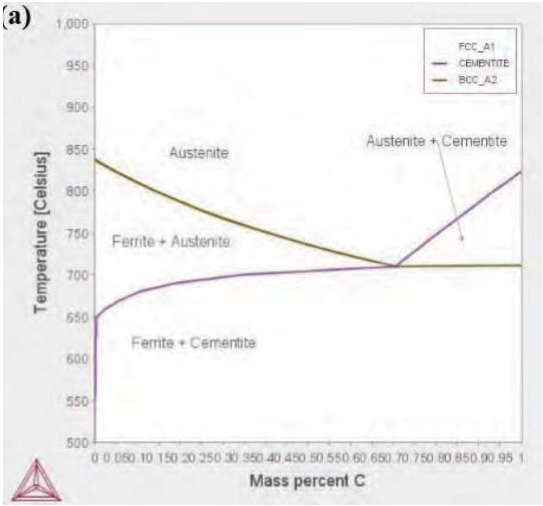

Figure 3. Thermo-Calc result window for equilibrium phase diagram for Steel chemistry

C. Annealing Simulation for Microstructure Tailoring

Following this, the specimens were isothermal annealed in the annealing simulator for 3 minutes at each of the inter-critical annealing temperatures (ICATs) of 700-750-800 °C and 850 °C. Then regulated cooling (via various cooling paths) as per CCT diagrams. A, B, and C cooling curves were derived from the annealing chamber thermocouple data logs and overlaid on the CCT diagrams as illustrated in Fig. 4.

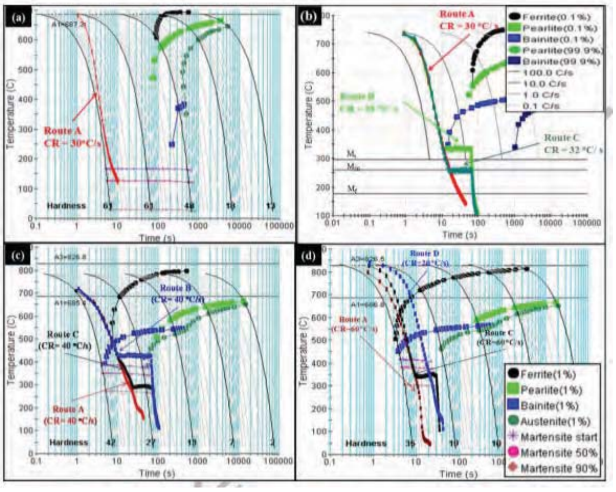

Figure 4. CCT diagrams with cooling curves superimposed for annealing temperature of (a) 700 ^{0}C (b) 750 ^{0}C (c) 800 0C (d) 850 ^{0}C

D. Simulation At 700 ^{0}C

For route A, the specimen was heated to 700°C, immersed for 3 minutes, and then cooled to room temperature at a rate of 30°C/s. The annealed specimen had ferrite and fine martensite laths. Heating and chilling created a necklace-like structure with recrystallized ferrite at the grain boundaries.

The optical micrograph revealed martensite and grain boundary ferrite. There was some remaining pearlite. Pearlite in the received steel recrystallized to ferrite during heating and soaking and phase transformed to austenite. The ferrite phase remained constant as austenite converted to martensite: ferrite (both original and recrystallized), martensite, and residual pearlite microstructure. Insufficient annealing temperature and duration reduced martensite. During inter-critical annealing of DP steel, ferrite recrystallization and austenite transformation compete and overlap. In the current study, coupling of these two processes happened at 700°C annealings. However, ferrite recrystallization was dominating, and austenite production was minor. The absence of austenite and hence martensite development prevented the creation of a suitable dual-phase structure following 700°C annealing. The other two procedures (B and C) were not used because austenite was found in tiny fractions at this annealing temperature.

E. Simulation At 750 ^{0}C

During annealing at 750°C, the cooling rates were 20–40°C/s. Route A was the same as 700°C. After 3 minutes of soaking at 750°C, the specimen was cooled at 35°C/s up to 350°C for route B. After 1 minute, the specimen was cooled to room temperature at a rate of 20°C/s. After 3 minutes of soaking at 750°C, the specimen was cooled at 32°C/s up to 250°C for route C. (martensitic region, identified). After 1 minute, the specimens were cooled to room temperature at a rate of 20°C/s. These three methods acquired the optical micrographs. Optical examination revealed ferrite and martensite phases with a 15% martensite volume percentage. There is evidence of partial austenite production and ferrite recrystallization-grain boundary recrystallization at 750°C. Austenite converted into fine-grained martensite upon further cooling along route A. Annulling at 750°C with cooling route A produced DP microstructure with ferrite and martensite phases.

A carbon redistribution occurred during the initial cooling (at 35 °C/s) up to 350 °C and subsequent holding in the bainitic zone for this approach. Some parts of austenite became carbon-rich, while others became carbon-deficient. Low carbon austenite became bainite (during holding at bainite region). Some carbon-rich austenite produced carbides during additional cooling (second cooling at 20 °C/s), while the rest formed martensite. A multiphase microstructure for cooling method C was expected, including ferrite, martensite, tempered martensite, bainite, and carbides. During the initial fast cooling (at 32 °C/s) along route C, austenite largely changed to martensite; on holding in the martensitic zone, this martensite received tempering and became tempered martensite. Carbon is predicted to permeate into untransformed austenite, stabilizing it. However, after a second cooling at 20 °C/s, part of the untransformed austenite converted into martensite, including carbides. During the soaking time, a highly saturated carbon solution was transformed into ferrite (route B).

F. Simulation At 800 ^{0}C

By Routes A, B, and C: Cooling rates of 20–40 °C /s were reached at an annealing temperature of 800 °C. For route A, a cooling rate of 40 °C /s was used. After three minutes of specified soaking at 800 °C, the specimen was cooled to about 400 °C (bainitic area) at a rate of 40 °C/s. After 1 minute, specimens were cooled to room temperature at a rate of 20 °C /s. After three minutes of soaking at 800 °C, the specimen was cooled to 280 °C (martensitic area) at a rate of 40 °C/s. After 1 minute, the specimen was cooled to room temperature at a rate of 20 °C /s. A dual-phase microstructure with a 20% martensite volume fraction was achieved by procedure A. Although the CCT diagram indicated the production of bainite, this phase combination was not detected in the steel specimen because of the lack of holding. A multiphase microstructure composed of ferrite, bainite, martensite, and traces of carbides was identified for route B. A multiphase microstructure including ferrite, conventional martensite, tempered martensite, and traces of bainite and carbides was reported for route C.

G. Simulation At 850 ^{0}C

By Routes A, C, and D: Cooling rates of 20–70 °C /s were reached at an annealing temperature of 850 °C. Three distinct specimens were annealed using three distinct cooling techniques (A, C, and D, respectively). Cooling pathway B (which was previously employed to induce bainite production) was omitted. This occurred because the bainitic zone in the CCT diagram migrated to the left at this inter-critical annealing temperature (ICAT = 850 °C). Additionally, the temperature range for bainitic transition was rather narrow. Thus, route B at 850 °C required an extremely rapid initial cooling rate prior to reaching isothermal holding in the bainite area. With such rapid cooling rates (and a short bainitic transformation range), it was challenging to manage regulated cooling while maintaining the proper transformation temperature range. Thus, in lieu of route B, a new (slow) cooling route D was established, consisting of continuous cooling at a rate of 20 °C /s. A cooling rate of 60 °C /s was used for route A. After three minutes of soaking at 850 °C, the specimen was cooled to 350 °C (martensitic area) at a rate of 60 °C/s. After 1 minute, the specimen was cooled to room temperature at a rate of 31 °C /s. After 3 minutes of soaking at 850 °C, the specimen was cooled to room temperature at a rate of 20 °C /s.

A dual-phase microstructure incorporating ferrite and martensite (37%) phases were discovered for route A. During cooling, the ferrite phase is comprised of both original ferrite and newly produced ferrite. The CCT diagram for 850 °C demonstrates that all cooling paths travel through the ferrite area, culminating in the transition of austenite to ferrite. This ferrite is referred to in this study as newly created ferrite to distinguish it from the ferrite that was in the steel prior to annealing. A multiphase microstructure incorporating ferrite (both original and freshly generated), martensite, tempered martensite, and a trace of bainite was expected for cooling route C. Following the initial cooling and subsequent retention in the martensitic zone, some carbon from newly created martensite seeped into untransformed austenite (leading in the development of tempered martensite) and enriched some parts of austenite. A piece of untransformed austenite (austenite with a low carbon content) converted into a bainite phase mixture. The untransformed austenite (austenite with a high carbon content) remained stable and converted to martensite during the second cooling [11, 12].

Carbides did not develop at this annealing temperature because to the rapid cooling rate (> 30 °C /s) used for the second cooling step after holding in the martensitic zone. The microstructure of route D consisted of ferrite (both original and newly produced), martensite, and bainite. Austenite first converted into ferrite, then into bainite, and lastly into martensite as it cooled.

V. CONCLUSIONS

Using inter-critical annealing process, a broad range of strength's combinations has been achieved. It is concluded that when hard phases like martensite, bainite, and others were present in the microstructure, they boosted UTS but decreased ductility and YS. Compared to route A, the presence of bainite may lower the UTS and raise the YS through route B. Route A provided the most strength, but at the sacrifice of ductility. Route C offered the optimum balance of strength and ductility. Annealing results achieved from annealing tests are much more accurate than those predicted by software. The differences are due to the fact that software projections are based on the premise of equilibrium heating, which is seldom seen during industrial heating. Additionally, cooling rates obtained by water quenching are much greater than those obtained under simulated circumstances. In samples annealed at 700, 750, and 800 °C, approach A resulted in significantly greater UTS and ductility than procedures B and C. This was ascribed to carbide production during pathways B and C. Due to the presence of carbides, ductility was reduced. Strength reduced due to these pathways (B and C) not resulting in the development of martensite fractions as route A did. The natural stress-strain curves (of the steel containing the DP structure at different annealing temperatures) acquired from actual tensile measurements were very consistent with the true stress-strain curves predicted by micromechanical modelling. As a result, it is stated that micromechanical modelling may be used to predict material behaviour without substantial experimental examination.

The greatest volume proportion of martensite obtained in this investigation was 37% at 850 °C through route A. Annealing tests may be expanded to higher temperature ranges in order to obtain a larger austenite content and hence a higher martensite proportion in order to analyze the change in mechanical characteristics. The research considered the influence of non-equilibrium heating, but only in a qualitative sense. Future research might involve determining the precise influence of heating rates on the microstructure by monitoring the heating rate throughout the austenitization process. The TRIP effect was not found to a substantial level in this investigation. Additional research may be undertaken with substantially longer holding durations to determine the TRIP impact.

REFERENCES

[1] Lesch, C., Kwiaton, N., & Klose, F. B. (2017). Advanced high strength steels (AHSS) for automotive applications− tailored properties by smart microstructural adjustments. Steel research international, 88(10), 1700210.

[2] Horvath, C. D. (2021). Advanced steels for lightweight automotive structures. In Materials, design and manufacturing for lightweight vehicles (pp. 39-95). Woodhead Publishing.

[3] Nanda, T., Singh, V., Singh, V., Chakraborty, A., & Sharma, S. (2019). Third generation of advanced high-strength steels: Processing routes and properties. Proceedings of the Institution of Mechanical Engineers, Part L: Journal of Materials: Design and Applications, 233(2), 209-238.

[4] Liu, Qinglong, Jeffrey Venezuela, Mingxing Zhang, Qingjun Zhou, and Andrej Atrens. "Hydrogen trapping in some advanced high strength steels." Corrosion Science 111 (2016): 770-785.

[5] Liu, L., He, B., & Huang, M. (2018). The role of transformation-induced plasticity in the development of advanced high strength steels. Advanced Engineering Materials, 20(6), 1701083.

[6] Seong, BS; Shin, E.J.; Han, Y.S.; Lee, C.H.; Kim, Y.J.; Kim, S.J. (2004) Effect of retained austenite and solute carbon on the mechanical properties in TRIP steels. Physica B, 350:

[7] Hulka, K. (2005) The Role of Niobium in Multiphase Steel, presented at METAL 2005, Germany 20-22 May, 2005.

[8] Fang, F., Lan, M. F., Lu, X., Zhang, Y. X., Wang, Y., Yuan, G. and Wang, G. D. (2017). The impact of niobium on the microstructure, texture and magnetic properties of strip-cast grain oriented silicon steel. Journal of Magnetism and Magnetic Materials, 442, 1-7.

[9] Zhao, J., Ma, L., Zayed, M. E., Elsheikh, A. H., Li, W., Yan, Q., & Wang, J. (2021). Industrial reheating furnaces: A review of energy efficiency assessments, waste heat recovery potentials, heating process characteristics and perspectives for steel industry. Process Safety and Environmental Protection, 147, 1209-1228.

[10] Thomas, G.A.; Speer, J.G.; Matlock, D.K. (2011) Quenched and Partitioned Microstructure Produced via Gleeble Simulations of Hot-Strip Mill Cooling Practices, Metallurgical and Materials Transactions A, 42A: 3652–3659.

[11] Kumar, G. N., & Reddy, G. B. (2017). Experimental Analysis on Nano-Based Phase Change Material for Cooling Applications in Tropical Buildings. *CVR Journal of Science and Technology*, *13*, 101-106.

[12] Rao, T. M., Srikar, N., Reddy, G. S., & Praveen, B. (2015). Ductility of Reinforced Concrete Beams. *CVR journal of Science and Technology*, *9*, 7-12.